Synthesis and Morphology of Segmented Poly (tetramethylene oxide)-Based Polyurethanes Containing Phosphonium Salts

ARTICLE *in* MACROMOLECULES · DECEMBER 2008

Impact Factor: 5.8 · DOI: 10.1021/ma801942f

4 AUTHORS, INCLUDING:

Wenqin Wang
University of Pennsylvania
19 PUBLICATIONS **206** CITATIONS

SEE PROFILE

Karen I Winey
University of Pennsylvania
331 PUBLICATIONS **11,291** CITATIONS

SEE PROFILE

Synthesis and Morphology of Segmented Poly(tetramethylene oxide)-Based Polyurethanes Containing Phosphonium Salts

Sharlene R. Williams,[†] Wenqin Wang,[‡] Karen I. Winey,[‡] and Timothy E. Long*,[†]

Department of Chemistry, Macromolecules and Interfaces Institute, Virginia Tech, Blacksburg, Virginia 24061 and Department of Materials Science and Engineering, University of Pennsylvania, Philadelphia, Pennsylvania 19104

Received August 27, 2008; Revised Manuscript Received September 27, 2008

ABSTRACT: A fundamental investigation of the influence of novel phosphonium bromide salts within the polymer main chain (23.75 mol %) of polyurethanes was conducted to elucidate the effect of ionic associations on hard segment hydrogen bonding. A novel poly(tetramethylene oxide) (PTMO)-based polyurethane containing a phosphonium diol chain extender was prepared using a conventional prepolymer method. In addition, a polyurethane containing a 1,4-butanediol chain extender was synthesized for comparison with the thermomechanical and morphological properties of the phosphonium ion-containing analog. Moreover, the unprecedented comparison of morphological development in the presence of cationic sites is described herein. Differential scanning calorimetry (DSC) revealed that phosphonium polyurethane was more crystalline compared to the noncharged analog, and it was presumed that enhanced hydrogen bonding in the noncharged polyurethane restricted polymer mobility and reduced PTMO crystallinity. Moreover, FT-IR spectroscopy demonstrated that hydrogen-bonding interactions were significantly reduced in the presence of phosphonium cations. These results correlated well with tensile properties, i.e., the noncharged polyurethane offered superior tensile strength compared to phosphonium polyurethane. X-ray scattering indicated that both polyurethanes were amorphous at room temperature and exhibited hard segment microphase separation. Upon stretching, the interparticle scattering between the microphase-separated domains aligned preferentially along the stretching direction. Scanning transmission electron microscopy (STEM) and energy-dispersive X-ray spectroscopy (EDS) in the STEM indicated that the charged polyurethane exhibited ionic aggregates that were rich in P and Br.

Introduction

Polyurethanes, which are often segmented block copolymers, consist of alternating hard and soft segments. The hard segments arise from reaction of an isocyanate with a low molecular weight diol chain extender, and the soft segments are typically derived from a low T_g polyol. Polyurethanes are useful thermoplastic elastomers due to their superior mechanical strength and elastomeric behavior that are derived from microphase separation and hydrogen bonding.[1] Polyurethanes are used in many applications such as abrasion-resistant components, biomaterials, durable coatings, and foams.[2−8] Polyurethane ionomers have also received attention as high-strength elastomers for biomedical[9,10] and conductive polymer[11−14] applications. Incorporation of ions into macromolecular structure causes formation of more complex morphological features, and ions potentially disrupt typical microphase separation in common polyurethanes.[15] Early reports of cation-containing polyurethanes typically involved postpolymerization functionalization to introduce quaternary ammonium groups.[16−18] Anionic polyurethanes, which commonly consist of either sulfonate or carboxylate groups in the hard segment, are typically more prevalent in the literature, and many researchers have modeled the presence of ionic aggregates within the microphase-separated polyurethane morphology.[19−23]

Dieterich et al. initially reviewed polyurethane ionomers in 1970.[16] Polyurethane ionomers continue to receive intense attention because of the potential synergistic interactions of hydrophobic soft segments, hydrogen-bonding groups, and ionic groups. At low ion concentrations incorporation of ionic groups into polyurethanes leads to water-dispersible products. However, many factors influence water dispersibility, including ion type, counterion, ion concentration, and soft segment composition.[24] With increasing attention to more environmentally friendly chemical syntheses and processing in the absence of volatile organic compounds (VOCs), ion-containing polyurethanes are attractive materials because water is the only solvent required for dispersion.[15,25] One potential limitation of water-dispersible polyurethanes is the hydrolytic instability of ester and urethane functional groups. However, Mequanint et al. determined that ionic domains "protected" the hydrophobic soft segments from hydrolytic degradation, depending on the polymer structure.[25] Specifically, their group revealed that polyurethanes containing ionic groups in the soft segment were more hydrolytically stable in aqueous solutions than analogs with ionic groups in the hard segment. Typically, water-dispersible polyurethanes contain either carboxylic acid or tertiary amine groups that are neutralized to their corresponding salts.[24]

Polyurethane ionomers offer unique mechanical properties due to the presence of ionic groups. The location of the ionic group and the ion content drastically influence the morphological and mechanical behavior of polyurethane ionomers. In some cases, ionic groups increase the degree of microphase separation and increase the tensile performance, but the results are highly dependent on polymer composition. For example, mechanical properties are especially dependent on whether the ionic groups are located in the hard or soft segment. Due to the expected hydrophilic nature of the ionic domains, water acts as a plasticizer and significantly influences the mechanical performance. Polyurethane ionomer research has expanded greatly in the past 30 years, and polymer structures are becoming more sophisticated. For example, Buruiana and co-workers synthesized poly(tetramethylene oxide) (PTMO)-based polyurethanes that contained a hard segment consisting of a novel, cationic stilbene diol based on 4-chloromethylphenylcarbamoyloxymethyl-*p*-stilbene.[26,27] Quaternary ammonium groups were also introduced for enhancing water dispersibility, while the stilbene

* To whom correspondence should be addressed. Phone: (540) 231-2480. Fax (540) 231-8517. E-mail: telong@vt.edu.
[†] Virginia Tech.
[‡] University of Pennsylvania.

10.1021/ma801942f CCC: $40.75
Published on Web 11/11/2008

group imparted interesting optical properties. Kim et al. synthesized polyurethane ionomers containing carboxylate ionic domains in polypropylene glycol soft segments.[28] The resulting polyurethanes possessed increased phase mixing and decreased solution viscosity and particle size.

The literature on phosphonium halide salt containing polymers is abundant; however, to our knowledge, researchers have not reported the synthesis of polyurethanes containing phosphonium groups in the hard segment. McGrath et al. reported the synthesis of poly(arylene ether) phosphonium ionomers for high-performance polymers in a variety of applications including ion-exchange membranes and conductive polymers.[29] However, in sharp contrast to our work, the phosphonium ionomers were prepared via reduction of polymeric phosphine oxides to phosphines in the presence of phenylsilane and subsequently quaternizing the phosphines with alkyl halides. Other researchers have reported the synthesis and characterization of phosphonium elastomers. Parent et al. synthesized poly(isobutylene-*co*-isoprene) phosphonium and ammonium elastomers that possessed dynamic mechanical behavior properties similar to ZnO-cured brominated poly(isobutylene-*co*-isoprene).[30] The rubbery plateau modulus was approximately 1×10^6 Pa, and the T_g values of all elastomers were similar, regardless of preparation. However, the solution behavior of the ionomers differed greatly compared to the noncharged elastomer that was covalently cross-linked with ZnO. The noncharged elastomer had a solution viscosity behavior that was independent of solvent selection; however, the influence of solvent polarity was discernible for the ionomers due to ionic aggregate formation and disruption. Soutar et al. reported another example of polyolefin-based elastomers that contained ionic groups. Living anionic polymerization techniques were used to prepare telechelic, phosphonium salt poly(butadiene)s with high 1,4-content. A temperature dependence of the ionic aggregate interactions was observed with dynamic mechanical thermal analysis, and the ionic aggregates dissociated at temperatures ranging from 70 to 120 °C.[31]

Previous work in our laboratories has focused on the structure−property relationships of linear and highly branched polyurethanes using a variety of soft segments, including poly(propylene glycol) (PPG) and poly(tetramethylene oxide) (PTMO).[1,32−38] Oligomeric $A_2 + B_3$ methodology was used to prepare branched polyurethanes, resulting in microphase-separated, low T_g segmented block polymers with excellent strain-hardening properties.[1,39] Recently, we demonstrated the synthesis of completely amorphous, highly branched poly(caprolactone)-based polyurethanes and poly(urethane urea)s that possessed dynamic mechanical behavior similar to a linear analog without difficulties attributed to the semicrystalline nature of poly(caprolactone).[39,40] In addition to highly branched and linear polyurethanes, we also prepared cross-linked Michael networks containing urethane functionality and investigated the effect of urethane sites on the thermomechanical performance. In particular, we ascertained the influence of polymer networks containing urethane linkages on the mechanical performance of poly(propylene glycol) (PPG)-based networks prepared via the carbon Michael addition reaction using acrylate and acetoacetate functionalities.[41] Urethane linkages improved the mechanical performance compared to non-hydrogen-bond-containing cross-linked networks, and synergistic effects were observed when the cross-link density was decreased while incorporating urethane segments. Previously, we also reported the influence of hydrogen bonding in photocross-linked star-shaped poly(D,L-lactide) (PDLLA) polymers that contained either methacrylate or urethane methacrylate functional groups on the periphery.[42,43] Both networks were highly cross-linked (>99%), but the tensile properties of the urethane methacrylate PDLLA networks were superior compared to the methacrylate PDLLA networks. The resulting PDLLA networks were promising high-performance bioadhesives.

Our group has also reported the potential advantages of phosphonium-salt-containing polymers. We previously reported the synthesis of phosphonium-based methacrylic ionomers using conventional free radical polymerization techniques. The resulting polymers formed free-standing ductile films, and the ionic interactions influenced the mechanical performance of the ionomer.[39] Furthermore, we recently reported the synergy of ionic interactions and hydrogen bonding where phosphonium salts containing a uracil hydrogen bond were blended with adenine-containing ABA triblock copolymers.[44] Novel adenine-containing triblock polymers were prepared via nitroxide-mediated polymerization, and these served as excellent templates for the nanoscale dispersion of uracil-containing phosphonium salts. Addition of the ionic guest altered the dynamic mechanical behavior and morphology compared to the polymer in the absence of the cationic phosphonium salt. It was concluded that the phosphonium salt was located in the adenine-containing blocks. X-ray scattering indicated a change in morphology from cylindrical to lamellar structure as the uracil-containing phosphonium salt was incorporated. ^{1}H NMR spectroscopy revealed complementary hydrogen bonding in the presence of the phosphonium salt.

In this work, urethane hydrogen bonding and phosphonium salt functionality were incorporated into the same polyurethane to elucidate the fundamental structure−property relationships of phosphonium-containing polyurethanes. This differs from the previous work described above, where the ionic group was the guest molecule and hydrogen bonding was based on more sophisticated complementary structures. Specifically, the effect of ionic interactions in a polyurethane hard segment on morphology and mechanical properties was elucidated using a variety of complementary analytical techniques. An appropriate noncharged polyurethane containing only urethane hydrogen-bonding interactions was prepared for comparison.

Experimental Section

Materials. PTMO oligomer (Terathane, Du Pont) with a number-average molecular weight of 2000 g/mol and 1,4-butanediol were purchased from Aldrich and dried in vacuo (0.1 mmHg) at 23 °C for 24 h prior to use. Bayer kindly provided bis(4-isocyanatocyclohexyl)methane (HMDI) with purity greater than 99.5%. Chloroform ($CHCl_3$, Fisher Scientific, Optima grade) was distilled from calcium hydride. Tetrahydrofuran (THF, EMD Science, HPLC grade), hexanes (Fisher Scientific, HPLC grade), dichloromethane (Fisher Scientific, HPLC grade), and diethyl ether (Fisher Scientific, 99.9%, anhydrous) were used as received. Dibutyl tin dilaurate (DBTDL, 99%) was dissolved in THF as a 1 wt % solution. A mixed solvent recrystallization was used to purify 1,4-bis(diphenylphosphino)butane (Aldrich, 98%) using hexanes and dichloromethane. Recrystallization was performed under nitrogen to minimize phosphine oxide formation. ^{31}P NMR spectroscopy revealed one peak after recrystallization. 2-Bromoethanol (Aldrich, 95%) was distilled prior to use.

Synthesis of Butane-1,4-bis[(2-hydroxyethyl)diphenylphosphonium] Bromide Chain Extender. In a two-necked, round-bottomed flask equipped with a stir bar and condenser 1,4-bis(diphenylphosphino)butane (5.694 g, 0.0134 mol) was introduced and purged under nitrogen. Chloroform (dry, 15 mL) and 2-bromoethanol (2.83 mL, 0.0401 mol) were subsequently syringed into the flask. The reaction was allowed to proceed at 60 °C for 24 h. The reaction product was precipitated into diethyl ether twice. The final product was obtained in 90% yield. ^{1}H NMR (400 MHz, CD_3Cl_3) δ = 7.56−7.80 (m, 20H), 5.36 (s, 2H), 3.88−3.97 (m, 4H), 3.46 (m, 4H), 3.19 (m, 4H), 1.99 (m, 4H). FAB MS: M + Br = 595.15 (found), molecular weight = 515.25 (calcd). Melting point = 123.8−124.1 °C.

Scheme 1. Synthesis of Butane-1,4-bis[(2-hydroxyethyl)diphenylphosphonium] Bromide Chain Extender

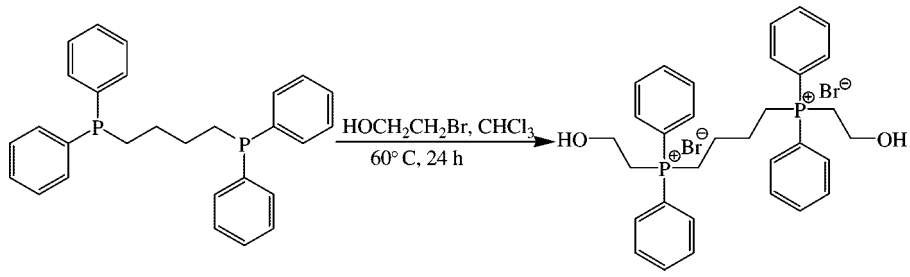

Synthesis of Polyurethanes. All reactions were conducted in three-necked, round-bottomed flasks that were equipped with an addition funnel, nitrogen inlet, and overhead stirrer. In the first step, HMDI end-capped PTMO prepolymers were prepared in the absence of solvent at 80 °C with 1 wt % DBTDL in THF (0.01 mL) as the catalyst.[1] In the second step, the chain extenders (butane-1,4-bis[(2-hydroxyethyl)diphenylphosphonium] bromide or 1,4-butanediol) were dissolved in $CHCl_3$ (20 wt % solids) and the polyurethanes prepared via dropwise addition (over 60 min) of the chain extender solution into the HMDI end-capped PTMO prepolymer. Polymerizations were allowed to proceed for 24 h at 80 °C, and the solutions remained homogeneous throughout polymerization. The polymer films containing butane diol chain extenders were optically clear; however, films containing butane-1,4-bis[(2-hydroxyethyl)diphenylphosphonium] bromide were opaque. Hard segment content was deduced using the following equation

$$\text{hard segment content} = 100[(\text{HMDI} + \text{chain extender})/(\text{HMDI} + \text{chain extender} + \text{PTMO})] \quad (1)$$

Characterization. ^{1}H NMR spectroscopy was utilized to determine monomer composition in $CDCl_3$ at 23 °C with a 400 MHz Varian UNITY spectrometer. FAB-MS was obtained on a JEOL HX110 dual-focusing mass spectrometer. A TA Instruments Hi-Res TGA 2950 with a temperature ramp of 10 °C/min in a nitrogen atmosphere was used for thermogravimetric analysis (TGA). Dynamic mechanical analysis (DMA) was conducted on a TA Instruments Q800 dynamic mechanical analyzer in tension mode at a frequency of 1 Hz and temperature ramp of 3 °C/min. The sample was cooled from room temperature to −30 °C prior to heating. The glass-transition temperature (T_g) was determined at the peak of the tan δ curve. Differential scanning calorimetry (DSC) was performed using a TA Instruments Q2000 differential scanning calorimeter under a nitrogen flow of 50 mL/min. The sample was first heated from −20 to 200 °C at a heating rate of 10 °C/min and held for 5 min to erase the thermal history. The cooling rate was 10 °C/min, and a subsequent heating from −130 to 200 °C at a heating rate of 5 °C/min was conducted. Dogbone-shaped film specimens, which were cut with a die according to ASTM D3368 specifications, were used for tensile tests performed on a 5500R Instron universal testing instrument with a cross-head speed of 50 mm/min using manual grips at 23 °C. The extent of hydrogen bonding of solvent-case films was evaluated using a MIDAC M2004 ATR-FTIR at ambient conditions. The spectra, including the background scan, were collected at a resolution of 4 cm^{-1}, and 128 scans were averaged. In all characterization methods great care was used in drying polymer samples before testing.

Morphological analysis was conducted using a variety of complementary techniques. X-ray scattering was performed on solvent-cast polyurethane films that were dried in vacuo (0.1 mmHg) at 60 °C for 24 h to ensure complete removal of $CHCl_3$. The multiangle X-ray scattering system (MAXS) used Cu X-ray from a Nonius FR 591 rotating-anode generator operated at 40 kV and 85 mA. The bright, highly collimated beam was obtained via Osmic Max-Flux optics and pin collimation in an integral vacuum system. The scattering data were collected using a Bruker Hi-Star multiwire detector with a sample to detector distance of 7, 11, 54, and 150 cm. The MAXS system provides an uncommonly wide range of scattering angles that was critical in evaluating the morphology of these segmented copolymers. The 2-D data reduction and analysis were performed using *Datasqueeze* software.[45] Scanning transmission electron microscopy (STEM) specimens were sectioned from solvent-cast and dried films using a Reichert-Jung ultramicrotome equipped with a cryo unit operated at −145 °C. Thin sections with nominal thickness of 50 nm were obtained with a dry diamond knife and transferred onto copper grids. The grids were stored in a vacuum desiccator at room temperature prior to imaging. STEM experiments were performed using a JEOL 2010F field emission scanning transmission electron microscope equipped with a Gatan Image Filter (GIF). High-angle annular dark field (HAADF) images were recorded with a 0.7 nm STEM probe at an accelerating voltage of 200 keV. X-ray energy-dispersive spectroscopy (EDS) experiments were performed in a JEOL 2010F, which is equipped with a Princeton Gamma Tech (PGT) X-ray energy-dispersive spectrometer and a Bruker digital processing unit. Spectra were acquired through placement of a stationary 0.7 nm probe at the point of interest and collecting a spectrum for 60 s. Data analysis was performed with the ESPRIT EDS Software.

Results and Discussion

A novel phosphonium diol chain extender was prepared from 1,4-bis(diphenylphosphino)butane and bromoethanol, as shown in Scheme 1. The resulting butane-1,4-bis[(2-hydroxyethyl-)diphenylphosphonium] bromide salt, which was purified after several precipitations into diethyl ether, was confirmed with ^{1}H NMR spectroscopy and FAB-MS. The salt was soluble in a variety of solvents including chloroform, methanol, and isopropanol but was insoluble in water. The salt was not classified as an ionic liquid since the melting point was above 100 °C (123.8−124.1 °C).

A novel ion-containing polyurethane was synthesized in a two-step process using 2000 g/mol PTMO as the soft segment, butane-1,4-bis[(2-hydroxyethyl)diphenylphosphonium] bromide as the chain extender, and HMDI as the diisocyanate (Scheme 2). The phosphonium-based polyurethane containing PTMO soft segments and HMDI was referred to as HMDI-P+(75)-2KPMTO. The prepolymer method was utilized to synthesize the novel polyurethane, and the first step involved the conventional preparation of an oligomeric HMDI end-capped PTMO.[1] After the reaction was cooled to room temperature, films were cast directly from the reaction mixture. For comparative purposes, a noncharged polyurethane containing a 1,4-butanediol chain extender was synthesized (HMDI-BD(75)-2KPMTO). The chemical compositions of both the ion-containing and the noncharged polyurethanes were similar. Each polymer had an equal concentration of hard segment on a mol % basis and a similar content on a wt % basis based on eq 1 in the Experimental Section. These values were calculated based on the charged amounts of reactants. HMDI-P+(75)-2KPMTO contained 75 mol % and 37 wt % hard segment, and HMDI-BD(75)-2KPMTO possessed 75 mol % and 24 wt % hard segment. Researchers have shown that using 1,4-butanediol as a chain extender resulted in polyurethanes that possessed excellent tensile properties and elasticity.[3] For this reason, 1,4-

Scheme 2. Synthesis of Phosphonium-Containing Polyurethanes (HMDI-P+(75)-2KPMTO)

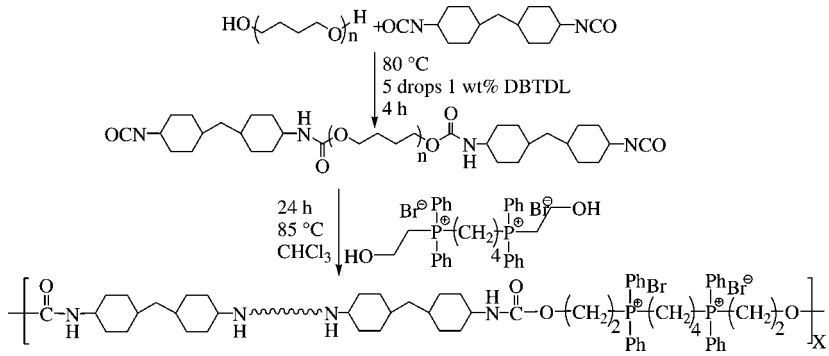

butanediol was utilized as the chain extender in the noncharged polyurethanes.

The water dispersibility of the ion-containing polyurethane was examined, and it was found that it was not dispersible in stirring water, even with heating to 60 °C. There are several possibilities for this occurrence, including the hydrophobic nature of PTMO soft segments. Furthermore, the ionic chain extender contained a substantial amount of hydrocarbon character, including phenyl rings, so the structure was perhaps too hydrophobic to promote water dispersibility of the polyurethane. In addition, since the molecular weight of butane-1,4-bis[(2-hydroxyethyl)diphenylphosphonium] bromide salt is relatively high for an ionic chain extender (515.25 g/mol), the ionic content of the polyurethane is greater than most ion-containing water-dispersible polyurethanes. For example, Yamada et al. reported incorporating 3 wt % of an ionic chain extender into water-dispersible polyurethanes.[46] The ionic content (23.75 mol %, 14 wt %) of the phosphonium polyurethane was perhaps too high, and ionic aggregation in solution prevented dispersion in water.

The HMDI-P+(75)-2KPMTO polyurethane had a T_d of 280 °C, and the HMDI-BD(75)-2KPMTO noncharged polyurethane had a slightly lower T_d of 263 °C according to TGA data. The difference in the thermal stabilities was considered insignificant since the error in TGA is approximately 2%, and the thermal stability difference between the two types of polyurethanes was only 17 °C.

DSC provided interesting information about crystallinity differences between the phosphonium bromide-containing and noncharged polyurethanes and confirmed many of the DMA results described below. Both DSC traces (Figure 1) are from the second heat in order to minimize effects of thermal history. The phosphonium polyurethane possessed crystallinity, and T_g, T_c, and T_m were observed at −79, −35, and 14 °C, respectively. Conversely, only a T_g at −78 °C was observed for the noncharged polyurethane. On the basis of this observation it appeared that hydrogen bonding restricted the mobility of the polymer chain and reduced the crystallinity of PTMO segment for the noncharged polyurethane. This was in agreement with Schneider et al., who reported that hydrogen bonding occurred between ether oxygens within the soft segment and urethane and urea units and thus hindered crystallization of the soft segment.[47] Moreover, the organic nature and bulkiness of the ionic groups suggested less dense packing of ionic groups in the aggregates; thus, the geometric constraint on the PTMO segments surrounding the ionic aggregates was much less than those traditional ionomers with metal cations.

Figure 2 summarizes the comparative dynamic mechanical behavior of the phosphonium-containing and noncharged polyurethanes, HMDI-P+(75)-2KPMTO and HMDI-BD(75)-2KPMTO. Both polymers showed similar PTMO soft segment T_gs with values ranging from −60 to −64 °C. This transition was higher than pure PTMO (−79 °C), which suggested some phase mixing. The greater glassy modulus of the phosphonium polyurethane indicated that the polymer had higher crystallinity, which was consistent with DSC as described above. This is in agreement with Wilkes et al., where they reported that the presence of PTMO crystals increased the glassy modulus.[48] A second transition that caused a decrease in the storage modulus occurred in the phosphonium-containing polyurethane at 47 °C, and this was attributed to melting of the crystalline PTMO segments.[47] The same transition occurred in the HMDI-BD(75)-2KPMTO polyurethane but to a much lesser extent since the decrease in modulus is very slight. The higher modulus in the

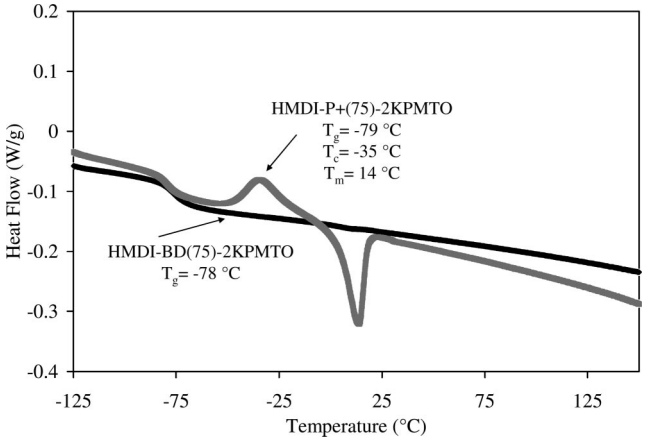

Figure 1. DSC traces for HMDI-P+(75)-2KPMTO (light gray) and HMDI-BD(75)-2KPMTO (black). Conditions: 5 °C/min, second heat.

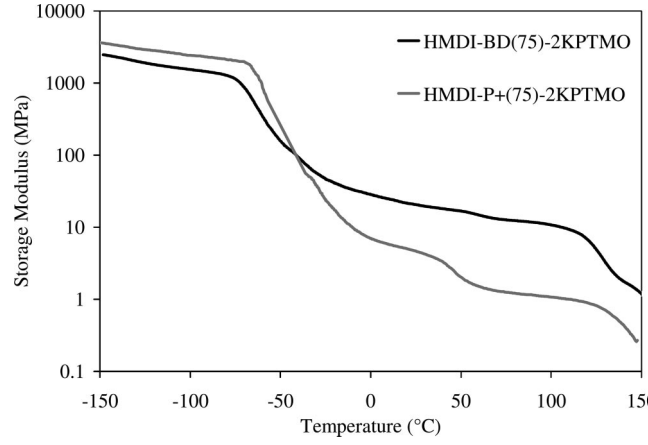

Figure 2. DMA curves demonstrating the transitions of the phosphonium-containing (gray line) and noncharged polyurethanes (black line). Conditions: 3 °C/min, 1 Hz, film tension mode.

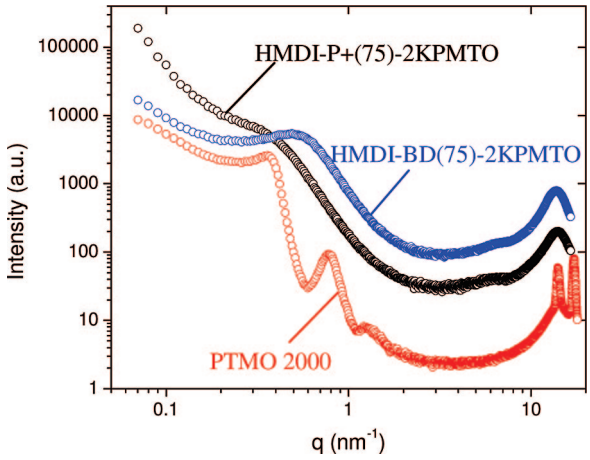

Figure 3. X-ray scattering intensity vs scattering vector (q) plotted in log−log scale for unstretched PTMO oligomer and unstretched PTMO-based polyurethane films containing different chain extenders.

rubbery plateau region (30 MPa) for the noncharged polyurethane suggested a greater extent of hydrogen bonding[49] in comparison to the phosphonium polyurethane, which had a lower rubbery plateau modulus (1 MPa). The lower plateau modulus could also suggest that the phosphonium polyurethane had a lower entanglement density,[50−52] which was possibly due to the presence of bulky aryl groups around the phosphonium cations. Both polymers possessed similar flow temperatures at ∼135 °C and retained a relatively flat rubbery plateau modulus prior to the onset of flow. It is interesting that both polyurethanes have similar flow temperatures, which indicated that the ionic aggregates persist to approximately the same temperature as the urethane hydrogen bonds.

Figure 3 shows the combined multiangle X-ray scattering data plotted in log−log scale. PTMO oligomers (M_n = 2000 g/mol) used in the synthesis of the polyurethanes were highly crystalline, showing two sharp crystalline reflection peaks at angular positions of 14 and 17 nm^{-1}, which corresponded to (020) and (110) peaks of PTMO crystals.[53] The PTMO oligomers also showed three crystalline lamellae−lamellae peaks at 0.36, 0.78, and 1.23 nm^{-1} that corresponded to a spacing of 16.3 nm. PTMO typically crystallizes into a monoclinic crystal structure with molecular chains having a planar zigzag conformation along the c axis of the unit cell.[54] The length of a fully extended, crystalline PTMO chain of 2000 g/mol is ∼16.8 nm, which is comparable to the interlamellar spacing measured via X-ray scattering.

The scattering data of both HMDI-P+(75)-2KPMTO and HMDI-BD(75)-2KPMTO displayed an amorphous peak at ∼14 nm^{-1} arising from PTMO soft segment.[53] In addition, both charged and noncharged polyurethanes also showed a weak broad peak at ∼6 nm^{-1} that was absent in the pure PTMO oligomer X-ray profile. This broad peak was attributed to the intramolecular scattering from the diisocyanate hard segments. The amorphous nature of both the soft and hard segments detected via X-ray scattering at room temperature was consistent with DSC results, which showed a T_m of PTMO at 14 °C for HMDI-P+(75)-2KPMTO and noncrystalline behavior of HMDI-BD(75)-2KPMTO. The crystallinity of hard segments is highly dependent on the structure and symmetry of diisocyanate groups.[55] Wilkes et al. previously showed that hard segments containing a kinked diisocyanate structure or a mixture of isomers, i.e., HMDI in this case, which are less able to form ordered crystalline structures,[56] as observed herein.

In addition to the two higher angle peaks, HMDI-BD(75)-2KPMTO also demonstrated a well-defined scattering peak at an angular position of ∼0.49 nm^{-1}, indicating microphase separation. This scattering peak was believed to arise from the interparticle scattering of hard domains with an average interdomain spacing of ∼12.8 nm in HMDI-BD(75)-2KPMTO. Others observed the incompatibility between soft and hard segments resulting in the formation of microphase-separated structures in various segmented polyurethane elastomers.[34,55−58] Small-angle X-ray scattering data also revealed a broad peak for HMDI-P+(75)-2KPMTO at a lower angle relative to the noncharged polyurethane, and this peak was less distinct due to the overlap with the small-angle upturn. The degree of microphase separation is highly dependent on the chemical composition. The HMDI-BD(75)-2KPMTO polyurethane did not possess bulky ionic groups in the middle of the urethane hard segments and thus had better packing of the hard segments to form well-defined microphase-separated domains. For the polyurethane-containing ionic groups there were two driving forces for microphase separation, namely, hydrogen-bonding interactions and ionic interactions. Additional experiments described below were conducted to clarify the morphology of the materials.

Scanning transmission electron microscopy (STEM) was applied to directly image the nanoscale morphology of HMDI-P+(75)-2KPMTO. The high-angle annular dark-field (HAADF) STEM image of HMDI-P+(75)-2KPMTO (Figure 4a) showed bright, circular ion-rich regions dispersed in dark, hydrocarbon-rich matrix. The mean diameter of STEM features was 43 ± 15 nm (Figure 4b), which was determined using Gaussian fits to line scans of intensity on >50 ionic aggregates. The size of ionic aggregates observed in STEM images was unexpected given the angular position of the broad X-ray scattering peak (Figure 3), which was ∼0.2−0.4 nm^{-1}. It is important to note that polyurethanes are potentially hydrophilic due to the presence of hydrogen bonds. Thus, the ultrathin films used for STEM imaging might have absorbed water after cryo-microtomy during grid transfer in ambient conditions. Any moisture would be difficult to remove under room temperature vacuum in the microscope. However, TGA analysis confirmed that our drying conditions adequately removed water from the samples within the error of TGA as discussed above. It is not expected that an organic cation, especially one with four phenyl rings and an alkylene spacer, would exhibit significantly more water retention. The extensive projection overlap in the STEM images and the diffuse boundary of the bright features also increased the error during measurement of the feature sizes. These ionic aggregates in the phosphonium polyurethane were much bigger than those observed in ion-containing vinyl polymers, such as poly(styrene-*ran*-sulfonated styrene) and poly(styrene-*ran*-methacrylic acid) copolymers neutralized with metal cations.[59,60] Previous STEM images of those solvent-cast ionomers have shown monodisperse, spherical ionic aggregates of 1−2 nm in diameters.[59,60] The large size of ionic aggregates observed here might have partially resulted from the bulkiness of the phosphonium ions, which each possess two phenyl groups. In addition, the rigid diisocyanate hard segments adjacent to the ionic groups may also participate in the observed ion-rich aggregates.

Energy-dispersive X-ray spectroscopy (EDS) was used to determine the elemental composition of ionic aggregates during STEM imaging (Figure 5). The spectra were collected by placing a focused electron beam of 0.7 nm diameter on bright and dark regions in the same field of view at high magnification to ensure similar thickness of the two locations. EDS results indicated that the bright, ion-rich region contained more Br and P elements in comparison to the matrix. A small amount of Br, P, and O elements were also detected in the dark matrix region. However, a definite conclusion was not made about whether there were any ionic groups dispersed in the matrix exclusively based on the EDS results due to the limited lateral resolution of EDS.

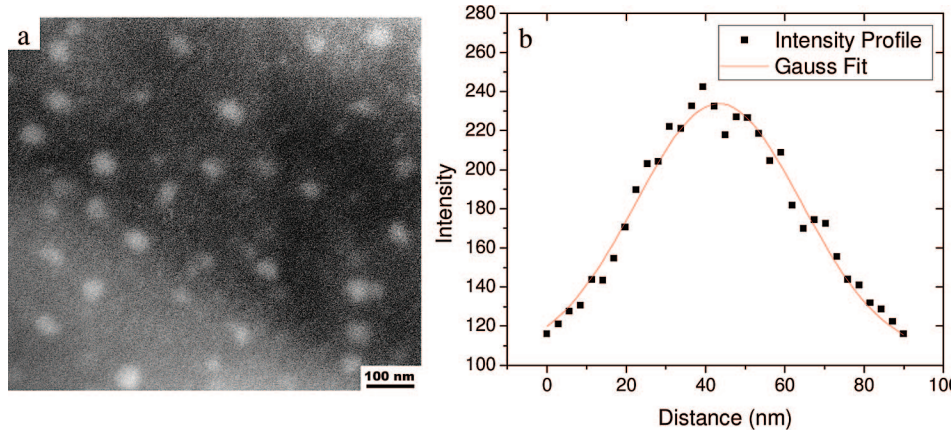

Figure 4. (a) HAADF STEM image of phosphonium polyurethane showed bright, spherical ion-rich regions dispersed in the dark, hydrocarbon-rich matrix. (b) Fitting the intensity profile across an isolated ionic aggregate with a Gaussian function provided the diameter of a STEM feature.

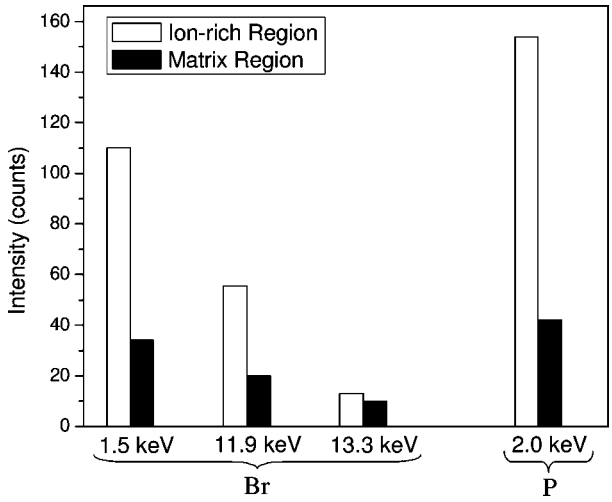

Figure 5. Spot EDS intensities taken from phosphonium polyurethane ultrathin films during STEM imaging with a stationary 0.7 nm probe placed on bright and dark regions in the specimen. The quantity of Br and P is greater in the bright ion-rich domains.

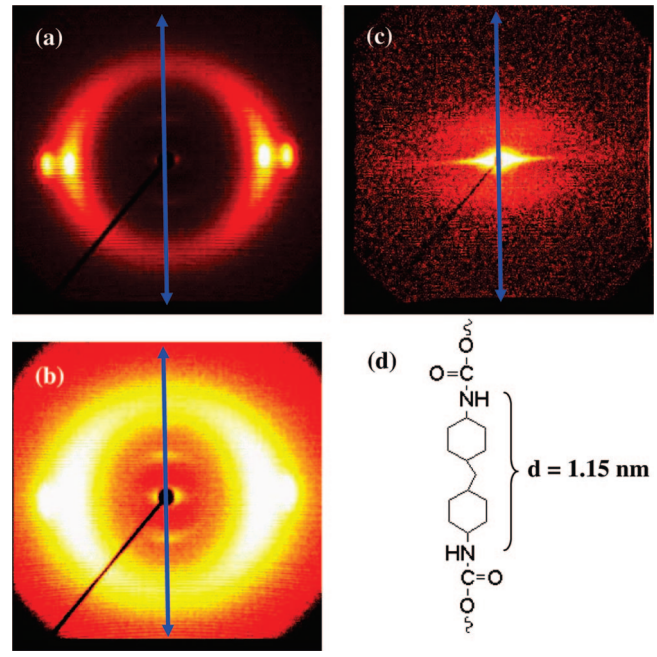

Figure 6. 2-D X-ray scattering patterns of the stretched HMDI-BD(75)-2KPMTO films at 600% strain. (a) Wide-angle pattern shows two equatorial scattering peaks at angular positions of 14 and 17 nm^{-1} that correspond to PTMO crystallization. (b) Same wide-angle pattern as in part a but in a different color scale to show the weak meridional reflections at 6 nm^{-1} that correspond to intramolecular scattering from hard segment. (c) Small-angle pattern shows meridional reflections at ~0.35 nm^{-1} that correspond to interparticle scattering from microphase-separated hard domains. The blue arrow indicates the stretching direction. (d) Chemical structure of the urethane segment in HMDI-BD(75)-2KPMTO.

To further refine the morphological description of the polyurethanes, the HMDI-BD(75)-2KPMTO film was stretched to ~600% strain at room temperature using a tensile testing instrument and studied via X-ray scattering in the stretched state. The 2-D wide-angle scattering pattern showed two equatorial scattering peaks at angular positions of 14 and 17 nm^{-1} (Figure 6a), which were the same as the crystalline reflection peaks of PTMO oligomers. Strain-introduced crystallization has been observed in various polymers.[61−63] Uniaxial stretching aligned the soft segment of the polymer backbone along the drawing direction, which effectively reduced the entropy of the polymer chain and promoted crystallization of the PTMO segment at room temperature. Furthermore, at high strain of 600% the intramolecular hydrogen bonding that restricted the mobility of PTMO segments was broken, thereby rendering more freedom for PTMO chain to reorganize into crystalline structures. Moreover, the 2-D wide-angle scattering pattern revealed weak meridional reflections at 6 nm^{-1} (Figure 6b), indicating alignment of the hard segment along the stretching direction. As shown previously in Figure 3, this peak at 6 nm^{-1} was absent in the PTMO oligomers. It was attributed to the urethane−urethane spacing along the backbone (Figure 6d). The peak position of 6 nm^{-1} corresponded to a real-space distance of 1.05 nm. The intramolecular distance between the two urethane groups was estimated to be 1.15 nm.[64] Stretching also introduced meridional scattering in the 2-D small-angle scattering pattern (Figure 6c), indicating that the orientation of the interparticle scattering between the microphase-separated hard domains was parallel to the stretching direction. Compared to the unstretched HMDI-BD(75)-2KPMTO, the peak position in the stretched film shifted from 0.49 to 0.35 nm^{-1}, signifying a larger spacing between the microphase-separated domains due to elongation of PTMO soft segments. Thus, uniaxial stretching altered the morphology in ways that were consistent with the proposed peak assignments. The intermolecular crystalline scattering signified PTMO chains crystallizing along the stretching direction. The intramolecular scattering from the hard segment also showed the alignment of hard segments along the stretching direction, and the interparticle scattering from the domains indicated that the

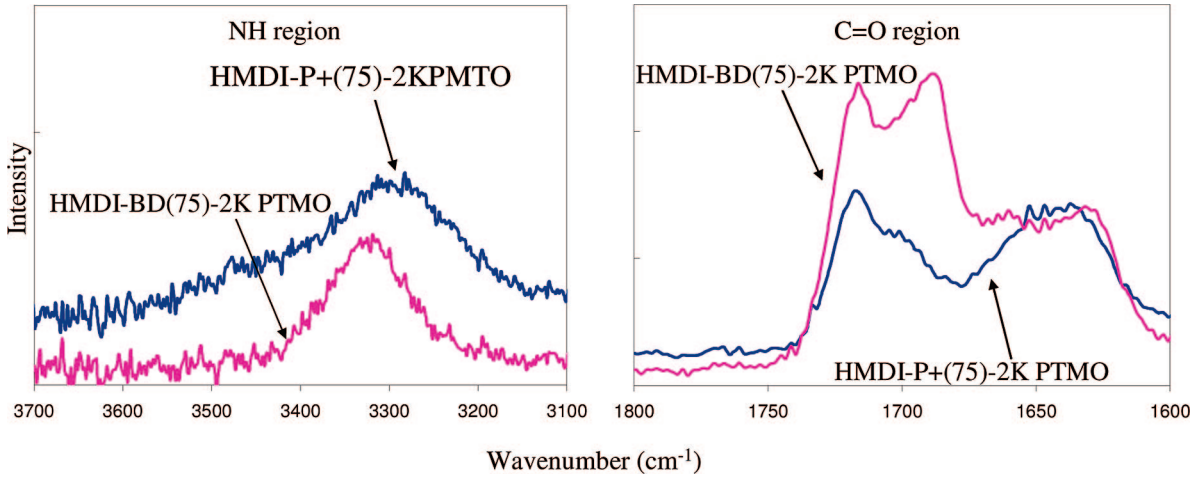

Figure 7. FT-IR spectroscopy of the NH (left) and C═O (right) region of HMDI-BD(75)-2KPMTO and HMDI-P+(75)-2KPMTO.

alignment of the microphase-separated domains was parallel to the stretching direction.

FT-IR spectroscopy was utilized to observe the extent of hydrogen bonding in both polyurethanes (Figure 7). Wilkes et al. demonstrated FT-IR spectroscopy was a simple and efficient means to determine the extent of hydrogen bonding in the carbonyl absorbing region of 1610−1760 cm^{-1} for noncharged polyurethanes.[65] Specifically, they confirmed that there are distinct peaks in the carbonyl region that are attributed to hydrogen-bond interactions for carbonyl groups. Non-hydrogen-bonded carbonyls have a peak at higher wavenumbers than hydrogen-bonded carbonyls. Furthermore, Wu et al. investigated the extent of hydrogen bonding in Nylon-6,6 in the presence of lithium salts.[66−68] They determined that the NH peak in the FT-IR spectrum narrows as the extent of hydrogen bonding increased. In the case of HMDI-BD(75)-2KPMTO and HMDI-P+(75)-2KPMTO, FT-IR spectroscopy was a very powerful tool to examine the extent of hydrogen bonding. As shown in Figure 7, the NH region is distinctly sharper for HMDI-BD(75)-2KPMTO than HMDI-P+(75)-2KPMTO. In addition, the carbonyl region of HMDI-BD(75)-2KPMTO had two peaks at 1716 and 1686 cm^{-1}. The peak at 1716 cm^{-1} was attributed to free carbonyl groups, and the peak at 1686 cm^{-1} was attributed to carbonyls that participated in hydrogen bonding. Clearly, a lack of hydrogen bonding was demonstrated for HMDI-P+(75)-2KPMTO, as evidenced with the absence of a peak in the hydrogen-bond carbonyl region at 1686 cm^{-1}. This demonstrated that the hydrogen-bonding interactions were significantly reduced due to the presence of ionic groups. As a result, ionic interactions were the primary driving force for microphase separation in the phosphonium polyurethane. Furthermore, this finding supported the tensile property results that are described below.

Representative stress−strain curves for both the phosphonium-containing and noncharged polyurethanes are shown in Figure 8. The charged and noncharged polyurethanes had comparable maximum elongation, which were 1330 ± 63% and 1170 ± 180%, respectively. The tensile stress at break was slightly higher for noncharged polyurethane (24.0 ± 1.2 MPa) comparing to HMDI-P+(75)-2KPMTO polyurethane (19.2 ± 1.1 MPa). It is important to note that all polyurethanes displayed excellent recovery after elongation. However, the presence of ionic groups disrupted hydrogen bonding and resulted in the slightly lower tensile performance of the phosphonium polyurethanes in comparison to the noncharged polymers. Interestingly, the tensile behavior after ~200% elongation was quite different as the HMDI-BD(75)-2KPMTO polyurethane displayed pronounced strain hardening behavior. The strain-induced crystallization was

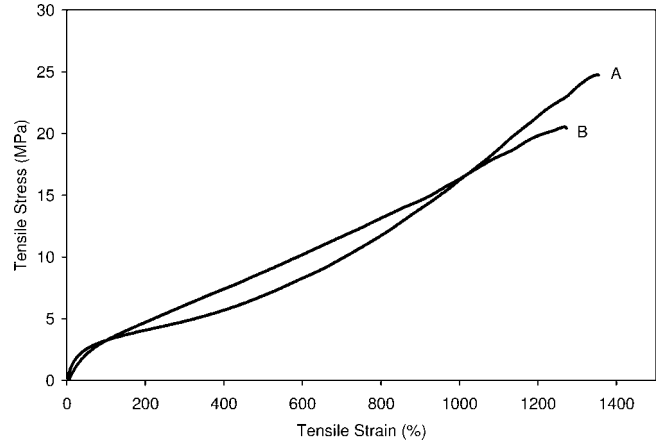

Figure 8. Comparison of the stress−strain behavior of linear, segmented, ion-containing polyurethane elastomer compared to the noncharged polyurethane: (A) HMDI-BD(75)-2KPMTO and (B) HMDI-P+(75)-2KPMTO.

confirmed previously with X-ray scattering (Figure 6a) and due to the recognized strain-induced crystallization of PTMO.[48,67,68] In addition, during uniaxial stretching it was speculated that the intramolecular hydrogen bonding between the ether oxygen in PTMO segments and the urethane group was broken and replaced with intermolecular hydrogen bonds,[69] which also increased the number of physical cross-links and resulted in the straining-hardening behavior. In contrast, the presence of disruptive ionic groups prevented an upturn in modulus for the phosphonium polyurethane. Repeated tensile experiments of the HMDI-P+(75)-2KPMTO polyurethane resulted in the reproducible behavior as shown in Figure 8.

Conclusions

A novel phosphonium-containing polyurethane was synthesized using a prepolymer method and characterized using a variety of methods. For comparative purposes, a polyurethane containing 1,4-butanediol as the chain extender was also synthesized. The noncharged PTMO-based polyurethane had hydrogen bonding as evident by FT-IR spectroscopy, while secondary bonding in the ion-containing polyurethane was dominated by the ionic interactions. Hydrogen-bonding interactions in HMDI-BD(75)-2KPMTO reduced chain mobility and crystallinity of the PTMO segment. DSC detected crystallization in HMDI-P+(75)-2KPMTO with a T_c (−30 °C) and a T_m (14 °C). At room temperature, X-ray scattering of both polyurethanes indicated that they were amorphous with scattering features corresponding to interparticle scattering

between microphase-separated hard domains (~0.2−0.5 nm^{-1}), intramolecular scattering from hard segments (~6 nm^{-1}), and intermolecular amorphous scattering at ~14 nm^{-1}. For the ion-containing polyurethane, STEM imaging confirmed the presence of ionic aggregates that were enriched with Br and P, although the observed size of aggregates was surprisingly large, perhaps due to their hydrophilic nature. X-ray scattering on stretched films verified the assignments of scattering peaks and detected strain-induced crystallization. Strain-induced crystallization was also observed in tensile testing, wherein HMDI-BD(75)-2KPMTO had an upturn in modulus at the high strain region. Both charged and noncharged polyurethanes exhibited excellent elasticity, high strain to break (>1100%), and high tensile strengths (>19 MPa). A future study will investigate the antimicrobial properties of these novel phosphonium polyurethanes. Furthermore, this type of phosphonium diol chain extender opens a wide field of potential research in polyurethane ionomers.

Acknowledgment. This material is based upon work supported by the U.S. Army Research Laboratory and the U.S Army Research Office under grant number W911NF-07-1-0452 Ionic Liquids in Electroactive Devices (ILEAD) MURI. The authors also thank Prof. Garth Wilkes and Dr. Sudipto Das for helpful discussions and assistance with FT-IR spectroscopic interpretations.

References and Notes

(1) Unal, S.; Yilgor, I.; Yilgor, E.; Sheth, J. P.; Wilkes, G. L.; Long, T. E. *Macromolecules* **2004**, *37* (19), 7081–7084.
(2) Woods, G. *The ICI polyurethanes book*; John Wiley: New York, 1990.
(3) Szycher, M. *Szycher's handbook of polyurethanes*; CRC Press: Boca Raton, 1999.
(4) Chattopadhyay, D. K.; Raju, K. V. S. N. *Prog. Polym. Sci.* **2007**, *32* (3), 352–418.
(5) Petrovic, Z. S.; Ferguson, J. *Prog. Polym. Sci.* **1991**, *16* (5), 695–836.
(6) Hepburn, C. *Polyurethane elastomers*, 2nd ed.; Elsevier Applied Science: London, 1992.
(7) Thomson, T. *Polyurethanes as specialty chemicals: principles and applications*; CRC Press: Boca Raton, 2005.
(8) *The polyurethanes book*; John Wiley: New York, 2002.
(9) Dickinson, R. B.; Nagel, J. A.; Proctor, R. A.; Cooper, S. L. *J. Biomed. Mater. Res.* **1997**, *36* (2), 152–162.
(10) Jeong, E. H.; Yang, H.; Youk, J. H. *Mater. Lett.* **2007**, *61* (18), 3991–3994.
(11) Krol, P.; Krol, B.; Subocz, L.; ruszkiewicz, P. *Colloid Polym. Sci.* **2006**, *285* (2), 177–183.
(12) Polizos, G.; Georgoussis, G.; Kyritsis, A.; Shilov, V. V.; Shevchenko, V. V.; Gomza, Y. P.; Nesin, S. D.; Klimenko, N. S.; Wartewig, S.; Pissis, P. *Polym. Int.* **2000**, *49* (9), 987–992.
(13) Shilov, V. V.; Shevchenko, V. V.; Pissis, P.; Kyritsis, A.; Georgoussis, G.; Gomza, Y. P.; Nesin, S. D.; Klimenko, N. S. *Mol. Cryst. Liq. Cryst.* **2001**, *361*, 269–274.
(14) Vatalis, A. S.; Kanapitsas, A.; Delides, C. G.; Viras, K.; Pissis, P. *J. Appl. Polym. Sci.* **2001**, *80* (7), 1071–1084.
(15) Reiff, H.; Dieterich, D. Urethane-based dispersions. In *Ionomers: Synthesis, Structure, Properties, and Applications*; Tant, M. R., Mauritz, K. A., Wilkes, G. L., Eds.; Blackie Academic and Professional: London, 1997; pp 444−501.
(16) Dieterich, D.; Keberle, W.; Witt, H. *Angew. Chem., Int. Ed.* **1970**, *9* (1), 40–50.
(17) Chen, S. A.; Hsu, J. S. *Polymer* **1993**, *34* (13), 2769–2775.
(18) Chen, S. A.; Hsu, J. S. *Polymer* **1993**, *34* (13), 2776–2782.
(19) Ding, Y. S.; Register, R. A.; Yang, C. Z.; Cooper, S. L. *Polymer* **1989**, *30* (7), 1204–1212.
(20) Register, R. A.; Cooper, S. L. *Abstr. Pap. Am. Chem. Soc.* **1989**, *197*, 203–POLYPOLY.
(21) Register, R. A.; Pruckmayr, G.; Cooper, S. L. *Macromolecules* **1990**, *23* (11), 3023–3026.
(22) Register, R. A.; Yu, X. H.; Cooper, S. L. *Polym. Bull.* **1989**, *22* (5−6), 565–571.
(23) Yang, C. Z.; Grasel, T. G.; Bell, J. L.; Register, R. A.; Cooper, S. L. *J. Polym. Sci., Part B: Polym. Phys.* **1991**, *29* (5), 581–588.
(24) Hourston, D. J.; Williams, G. D.; Satguru, R.; Padget, J. C.; Pears, D. *J. Appl. Polym. Sci.* **1999**, *74* (3), 556–566.
(25) Mequanint, K.; Sanderson, R. *Eur. Polym. J.* **2006**, *42*, 1145–1153.
(26) Buruiana, E. C.; Buruiana, T.; Strat, G.; Strat, M. *J. Polym. Sci., Part A: Polym. Chem.* **2002**, *40* (11), 1918–1928.
(27) Buruiana, T.; Buruiana, E. C. *J. Polym. Mater.* **2001**, *18* (1), 97–102.
(28) Kim, B. K.; Yang, J. S.; Yoo, S. M.; Lee, J. S. *Colloid Polym. Sci.* **2003**, *281*, 461–468.
(29) Ghassemi, H.; Riley, D. J.; Curtis, M.; Bonaplata, E.; McGrath, J. E. *Appl. Organomet. Chem.* **1998**, *12*, 781–785.
(30) Parent, J. S.; Penciu, A.; Guillen-Castellanos, S. A.; Liskova, A.; Whitney, R. A. *Macromolecules* **2004**, *37* (20), 7477–7483.
(31) Lindsell, W. E.; Radha, K.; Soutar, I.; Stewart, M. J. *Polymer* **1990**, *31* (7), 1374–1378.
(32) Fornof, A. R.; Glass, T. E.; Long, T. E. *Macromol. Chem. Phys.* **2006**, *207* (14), 1197–1206.
(33) McKee, M. G.; Park, T.; Unal, S.; Yilgor, I.; Long, T. E. *Polymer* **2005**, *46* (7), 2011–2015.
(34) Sheth, J. P.; Unal, S.; Yilgor, E.; Yilgor, I.; Beyer, F. L.; Long, T. E.; Wilkes, G. L. *Polymer* **2005**, *46* (23), 10180–10190.
(35) Sheth, J. P.; Wilkes, G. L.; Fornof, A. R.; Long, T. E.; Yilgor, I. *Macromolecules* **2005**, *38* (13), 5681–5685.
(36) Supriya, L.; Unal, S.; Long, T. E.; Claus, R. O. *Chem. Mater.* **2006**, *18* (10), 2506–2512.
(37) Yilgor, I.; Mather, B. D.; Unal, S.; Yilgor, E.; Long, T. E. *Polymer* **2004**, *45* (17), 5829–5836.
(38) Lepene, B. S.; Long, T. E.; Meyer, A.; Kranbuehl, D. E. *J. Adhes.* **2002**, *78* (4), 297–312.
(39) Unal, S. Synthesis and characterization of branched macromolecules for high performance elastomers, fibers, and films, Ph.D. Thesis, Virginia Tech, Blacksburg, VA, **2005**.
(40) Unal, S.; Ozturk, G.; Sisson, K.; Long, T. E. *J. Polym. Sci., Part A* **2008**, 6285–6295.
(41) Williams, S. R.; Mather, B. D.; Miller, K. M.; Long, T. E. *J. Polym. Sci., Part A: Polym. Chem.* **2007**, *45* (17), 4118–4128.
(42) Karikari, A. S.; Edwards, W. F.; Mecham, J. B.; Long, T. E. *Biomacromolecules* **2005**, *6* (5), 2866–2874.
(43) Karikari, A. S.; Williams, S. R.; Heisey, C. L.; Rawlett, A. M.; Long, T. E. *Langmuir* **2006**, *22* (23), 9687–9693.
(44) Mather, B. D.; Baker, M. B.; Beyer, F. L.; Green, M. D.; Berg, M. A. G.; Long, T. E. *Macromolecules* **2007**, *40*, 4396–4398.
(45) Heiney, P. A. *Comm. Powder Diffr. Newslett.* **2005**, *32*, 9–11.
(46) Chinwanitcharoen, C.; Kanoh, S.; Yamada, T.; Hayashi, S.; Sugano, S. *J. Appl. Polym. Sci.* **2004**, *91*, 3455–3461.
(47) Hu, C. B.; Ward, R. S.; Schneider, N. S. *J. Appl. Polym. Sci.* **1982**, *27* (6), 2167–2177.
(48) Das, S.; Yilgor, I.; Yilgor, E.; Inci, B.; Tezgel, O.; Beyer, F. L.; Wilkes, G. L. *Polymer* **2007**, *48*, 290–301.
(49) Christenson, C. P.; Harthcock, M. A.; Meadows, M. D.; Spell, H. L.; Howard, W. L.; Creswick, M. W.; Guerra, R. E.; Turner, R. B. *J. Polym. Sci., Part B: Polym. Phys.* **1986**, *24* (7), 1401–1439.
(50) Fetters, L. J.; Lohse, D. J.; Graessley, W. W. *J. Polym. Sci., Part B: Polym. Phys.* **1999**, *37* (10), 1023–1033.
(51) Llorens, J.; Rude, E.; Marcos, R. M. *J. Polym. Sci., Part B: Polym. Phys.* **2000**, *38* (11), 1539–1546.
(52) Wang, D. H.; Shen, Z. H.; Guo, M. M.; Cheng, S. Z. D.; Harris, F. W. *Macromolecules* **2007**, *40* (4), 889–900.
(53) Sun, Y.; Jeng, U.; Huang, Y.; Liang, K.; Lin, T.; Tsao, C. *Physica B* **2006**, *385*, 650–652.
(54) Tadokoro, H. *J. Polym. Sci., Part C* **1966**, *15*, 1–15.
(55) Aneja, A.; Wilkes, G. L. *Polymer* **2003**, *44* (23), 7221–7228.
(56) Klinedinst, D. B.; Yilgor, E.; Yilgor, I.; Beyer, F. L.; Wilkes, G. L. *Polymer* **2005**, *46* (23), 10191–10201.
(57) O'Sickey, M. J.; Lawrey, B. D.; Wilkes, G. L. *Polymer* **2002**, *43* (26), 7399–7408.
(58) Sheth, J. P.; Klinedinst, D. B.; Wilkes, G. L.; Iskender, Y.; Yilgor, E. *Polymer* **2005**, *46* (18), 7317–7322.
(59) Benetatos, N. M.; Chan, C. D.; Winey, K. I. *Macromolecules* **2007**, *40* (4), 1081–1088.
(60) Zhou, N.; Chan, C. D.; Winey, K. I. *Macromolecules* **2008**, 41.
(61) Martins, C. I.; Cakmak, M. *Polymer* **2007**, *48* (7), 2109–2123.
(62) Bartczak, Z.; Kozanecki, A. *Polymer* **2005**, *46* (19), 8210–8221.
(63) Klimov, E.; Hoffmann, G. G.; Gumenny, A.; Siesler, H. W. *Macromol. Rapid Commun.* **2005**, *26* (13), 1093–1098.
(64) The distance is calculated based on the size of cyclohexane (0.45 nm) and the carbon−carbon bond length of 0.145 nm with a bond angle of 120°.
(65) Yilgor, I.; Yilgor, E.; Guler, I. G.; Ward, T. C.; Wilkes, G. L. *Polymer* **2006**, *47*, 4105–4114.
(66) Wu, Y.; Xu, Y.; Wang, D.; Zhao, Y.; Weng, S.; Xu, D.; Wu, J. *J. Appl. Polym. Sci.* **2004**, *91*, 2869–2875.
(67) Das, S.; Cox, D. F.; Wilkes, G. L.; Klinedinst, D. B.; Yilgor, I.; Yilgor, E.; Beyer, F. L. *J. Macromol. Sci., Part B* **2007**, *46* (5), 853–875.
(68) Feng, D.; Wilkes, G. L.; Leir, C. M.; Stark, J. E. *J. Macromol. Sci., Part A: Chem.* **1989**, *26* (8), 1151–1181.
(69) Myung, D.; Koh, W.; Ko, J.; Hu, Y.; Carrasco, M.; Noolandi, J.; Ta, C. N.; Frank, C. W. *Polymer* **2007**, *48*, 5376–5387.

MA801942F